Investigation of corrosion behaviour of carbon steel in simulated soil solution from anodic component of polarisation curve

IOP Conf. Series: Materials Science and Engineering **430** (2018) 012039 doi:10.1088/1757-899X/430/1/012039

Investigation of corrosion behaviour of carbon steel in simulated soil solution from anodic component of polarisation curve

Phumlani Mjwana[1, 2, a] Mandla Mahlobo[1, 2, b] Obadele Babatunde[1, c] Philippe Refait[2, c] Peter Olubambi[1, e]

[1] Centre for Nanoengineering and Tribology, University of Johannesburg, Corner of Siemert and Beit Streets, Johannesburg, Gauteng, 2094 South Africa
[2] Laboratoire des Sciences de l'Ingénieur pour l'Environnement (LaSIE), UMR 7356 CNRS-Univ. La Rochelle, Bât. Marie Curie, Av. Michel Crépeau, F-17042 La Rochelle cedex 01 France

[a] mjwanap@gmail.com

Abstract. Marine structures and buried pipelines are constantly exposed to extreme conditions with elements such as temperature variation, soil ion content, dissolved metals, etc posing a continuous threat on the integrity and lifespan of the structures. Quantification of these elements has been limited to studying only a few of the parameters, with the resulting corrosion behaviour not fully understood. The purpose of this study was to investigate the corrosion behaviour of carbon steel in simulated soil solution using the anodic component attained from modelled polarisation curves. The behaviour of the metal/electrolyte interface was studied using non-invasive in-situ electrochemical techniques at OCP. A combination of voltammetry, electrochemical impedance spectroscopy with X-ray diffraction analysis of the mineral layer were utilised. The expression for the anodic component of the current as a function of potential was attained from $\log|j_a|$ vs. potential plots. Mathematical modelling of the experimental polarisation curves was done using *OriginPro Data Analysis & Graphing Software*. Results showed that at OCP, lepidocrocite, carbonated green rust, calcite and aragonite were found as the corrosion process involved anodic and cathodic zones. Voltammetry around OCP (VAOCP) and linear polarisation resistance (LPR) showed the necessity for corrosion protection as the adopted electrochemical system resulted in a progressively corrosive environment. Kinetics and mechanism of the anodic and cathodic process indicated corrosion processes similar to aerated soil conditions.

1. Introduction

Buried pipelines are continuously exposed to harmful and threatening elements in the immediate surrounding soil environment such as soil moisture, temperature variation, pH, soil ion content, dissolved metals, etc. all of which could prove detrimental to the service life of buried pipelines [1]. To protect these pipelines from external corrosion, a combination of organic coatings and cathodic protection (CP) is used. According to the EN 12954: 2001 standard, a residual corrosion rate lower of equal to 10 µm/y must be maintained. Application of CP in immersed conditions containing calcium and magnesium results in the formation of calcareous deposits. While this layer has been shown to have a beneficial effect for CP [2], the role has never been quantified

Cathodic protection (CP) is one of the most common and effective means for corrosion prevention in offshore metallic facilities and buried carbon steel structures [3,4]. CP leads to scaling of which, in saline fluids transportation industries such as oil recovery, power generation and water desalination may lead to major problems [5]. There remains a beneficial effect of the scaling in CP in terms of

corrosion protection [6]. The scaling deposit often contain calcium carbonate in the form of calcite and/or aragonite with brucite precipitating at low applied potentials.

It has been demonstrated that high temperature, more cathodic potentials and increased interfacial pH are the real driving forces of the precipitation of brucite [6]. It was further shown that the brucite layer acts as an inhibitor for the $CaCO_3$ aragonite deposition as the initial scaling process occurs between the brucite crystals. Instantaneous crystallization of $CaCO_3$, independent of applied potential, was shown by optical microscope in a study in artificial water [7]. The same study illustrated the inhibiting effect of SO_4^{2-} of which modified the calcite morphology under cathodic polarization. One of the most crucial parameters that influences the metal/electrolyte residual corrosion behaviour is O_2 at the vicinity of the electrode.

The present study focuses on the interactive behavior of carbon steel and O_2 in a corrosive environment and studies the corrosion behavior at the metal/electrolyte interface

2. Experimental procedure

The S235JR carbon steel was used in the present study is commonly used for pipelines and construction of buildings and bridges [8]. Its average composition (weight %) was: 98.94% Fe, 0.097% C, 0.49% Mn, 0.020% P, 0.09% Si, 0.05% Cr, 0.11% Ni, 0.16% Cu, and 0.042% S. Cylindrical coupons (15 mm diameter, 6 mm thick) were cut from the same sheet, polished with silicon carbide grade P600, rinsed with acetone and rapidly dried in an air flow. Coupons were connected by welding to copper wire, embedded in epoxy resin and studied at the end of each experiment for analysis of deposit layer and corrosion products. Only one surface of the coupon, with total area 1.77 cm^2, was exposed to the simulated soil solution. A single coupon was immersed in 750ml simulated solution in each electrochemical cell with platinum plate and saturated calomel electrode (SCE) used as the counter and reference electrode respectively. The solution was gently stirred and the beaker top left uncovered and thus exposed to the atmosphere.

Table 1. Mineral composition of Electrolyte 1 as prepared on the day of each experiment

Compounds	**Composition (*mmol/l*)**
NaCl	10
$CaCl_2 \cdot 2H_2O$	2
$MgCl_2 \cdot 6H_2O$	1
$Na_2SO_4 \cdot 7H_2O$	1.5
$NaHCO_3$	2

The simulated soil solution was prepared using analytical grade reagents. All experiments were conducted in soil simulated solution containing main species present in soil as determined by ASTM norm D1141 (American Society for Testing Materials) represented in Table 1. Prepared using analytical grade reagents, Electrolyte 1 (Table 1) was used as the calcareous deposit forming solution. Electrolyte 1 was used for all experiments unless otherwise stated.

Voltammetry around OCP (VAOCP) could be used as a non-destructive technique in order to monitor the evolution with time of the residual corrosion behavior [9]. It includes a moderate potential range (±50 mV in the present study) which is assumed sufficient to have a negligible damage on the metal/electrolyte interface. The fitting procedure of the experimental polarization curve used for the present study was adapted from Akkouche et al. [10] in order to determine the controlling corrosion kinetics [11]. A scan rate $dE/dt = 0.1\ mVs^{-1}$ was used.

In order to obtain the polarization curves around OCP, the potential was swept from OCP to OCP +50mV (forward scan) and then from OCP +50mV to OCP –50mV (reverse scan). During VAOCP experiments potential range was ±50mV unless stated otherwise. For CP experiments the above mentioned procedure necessarily modifies the metal/electrolyte interface. For this reason, the forward scan gives the true nature of the metal/electrolyte interface. The corrosion potential (E_{corr}) was directly read on the log|j| vs. E_{IRfree} curve while corrosion current density (j_{corr}), the Tafel coefficients β_a and β_c, and the limiting current density (j_{lim}) were obtained from the computer fitted curve. Polarization curves were attained at day 2 and day 7.

A true representation of the corrosion behavior was obtained from the anodic component of the modelled polarization curves. For this study, the anodic component was compared for forward scans at day 7 by extrapolating the current density value at the applied potential for the respective potential [12]. This would give a true reflection of the residual corrosion rate (V_{CR}). It remains true that cathodic polarization protected the electrode from corrosion. There was a residual corrosion behavior that may be observed and quantified [12,13]. As a basis and point of reference, the anodic component was also evaluated for modelled polarization curves at OCP.

X-ray diffraction (XRD) experiments were carried out at room temperature with an INTEL XRD Equinox 6000 in a step mode scanning using Co-Kα

3. Results and discussion

With the many parameters involved in the electrochemical system, the path travelled by current is one of the most crucial. Ohm's law takes into account the electric current flow between two points and the resistance of the path. With resistance being one of the major components, the Ohmic drop or IR drop has to be taken into account because the measured potential is influenced by the resistance of the simulated soil, metallic path and/or corrosion products. Electrochemical impedance spectroscopy (EIS) was conducted to examine the high frequency behaviour at OCP and thus determine the IR drop. The system OCP ($E_{OCP} = –0.69V_{SCE} \pm 0.02V_{SCE}$) was monitored for 7 days and the system allowed to reach steady state before EIS was conducted. The impedance data (Figure 1) reveals a R_e value of 110 Ω.

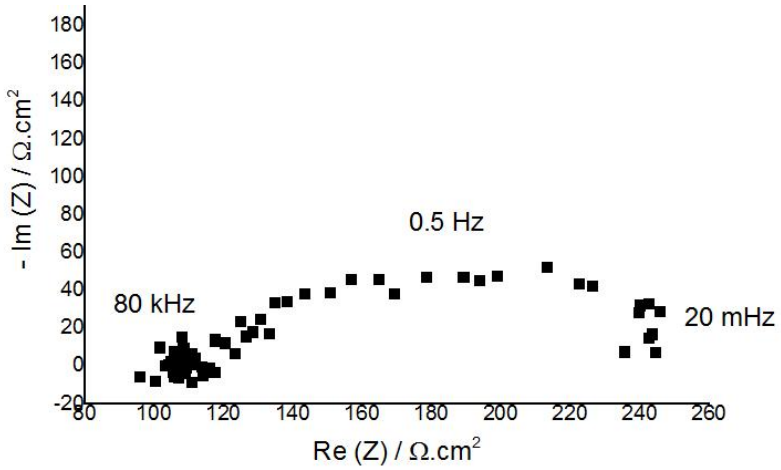

Figure 1. Nyquist plot at OCP

3.1. Polarisation resistance

Linear polarisation resistance (LPR) was performed at day 2 and day 7 to assess the corrosion behaviour of the electrode at the metal/electrolyte interface [9]. Polarisation resistance (R_P) could be determined by finding the gradient of the current density vs potential line at zero current (Figure 2). At current density zero there was no current flowing and the respective potential was taken as the free corrosion potential (E_{corr}). It was at this point where R_P was best represented. Therefore the inverse of the gradient was the polarization resistance with units Ohm squared centimetre (Ω.cm^2). R_P values determined were 1301.7 Ω.cm^2 and 1210.8 Ω.cm^2 for day 2 and day 7 respectively. These values were a direct indication of the resistance as to polarisation of the metal, in the respective electrolyte, against corrosion with respect to time. It can be deduced that the decrease of R_P indicated a reduction of corrosion resistance with time. Therefore a higher corrosion rate was expected and thus a greater need for corrosion protection. This also has a direct link to the increase of potential observed in Figure 2 which points towards formation of corrosion products.

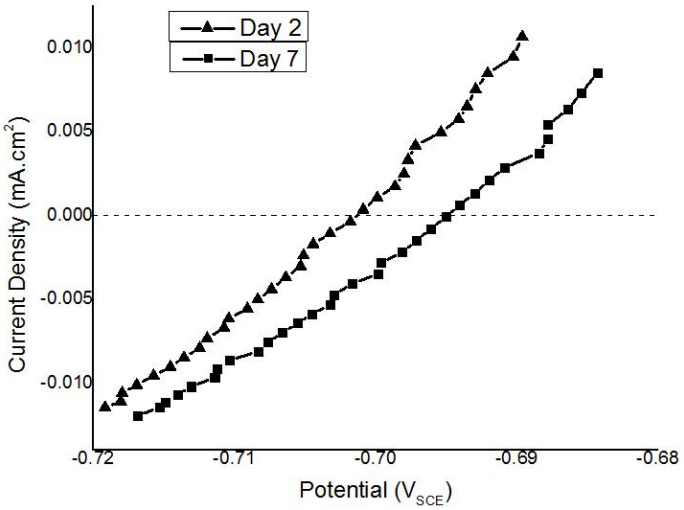

Figure 2. Linear polarisation resistance plot for day 2 and 7 of OCP experiment

3.2. Open circuit potential

The free corrosion potential (E_{OCP}) for the system was determined by allowing the electrochemical cell to reach a steady state (see Figure 3). No current or potential was applied. The potential starts off at a high value of –0.48 V_{SCE}. This potential corresponds to the oxide film formed as a result of iron oxidation in the atmosphere. As the oxide film dissolves, the potential decreases. The potential reaches its lowest point after a single day of –0.70 V_{SCE}. Over the seven day period the potential plateaus at an averages value of –0.69 V_{SCE}.

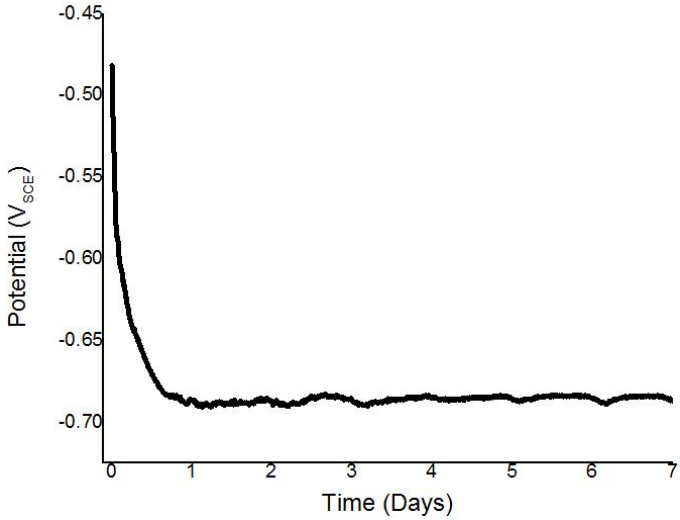

Figure 3. OCP evolution monitored over 7 days.

3.3. Voltammetry and corrosion rates

The kinetics and mechanism of the anodic and cathodic processes at OCP was done using VAOCP with potential range of ±50 mV [10]. VAOCP is able to get information about the electrochemical system while inducing minimal damage to the metal/electrolyte interface. The controlling kinetic model of the electrochemical system had to be determined according to the best computed fit when compared to the experimental data. Kinetic models include charge transfer (tafel), mixed activation/diffusion (mixed), diffusion control (diffusion) and a combination of H_2O and O_2 reduction control (hydroevolution) [10]. The anodic controlling mechanism was assumed to be charge transfer and this is an assumption that is carried throughout the study. This can be observed from Figure 4, and the modelled curves to follow, that the anodic experimental and computed curve are best fitted with a straight line, which indicates Tafel law behaviour.

The parameters determined by the mathematical model were as follows; current density (j_{corr}), tafel coefficients (β_a and β_c), limiting current density (j_{lim}) and E_{corr}. E_{corr} is determined graphically from the log current density vs potential plot and then fixed when the model was run. E_{corr} increases from – 0.70 V_{SCE} at day 2 to – 0.68 V_{SCE} at day 7 (not shown), which may be attributed to the formation of a corrosion layer on the surface of the metal as mentioned above. Although anodic and cathodic potentials were applied, the VAOCP method did not influence the corrosion of steel because E_{corr} values were close to E_{OCP}.

With a Chi Square (R^2) value of above 0.999 for all modelled curves, this method of kinetic modelling gave a range of parameter values for a single experimental curve. For example, day 7 curve parameter values for mixed controlling reaction βa ranged from 15 V^{-1} to 33 V^{-1}, with β_c deviating inconsistently as well. This issue was resolved by increasing the potential range for VAOCP to ±100 mV at the end of the experiment (day 7), while maintaining the range at ±50 mV at day 2 in order to limit the interfacial perturbation.

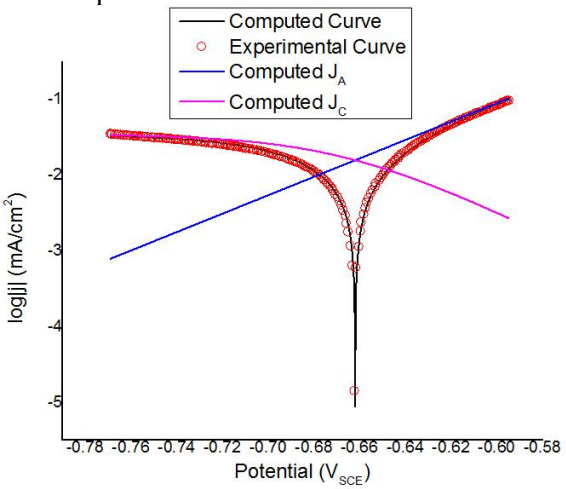

j_{corr} (mA/cm²)	0.021 ± 0.002
β_a (V^{-1})	28 ± 1
β_c (V^{-1})	-25 ± 4
j_{lim} (mA/cm²)	-0.040 ± 0.006
E_{corr} (V_{SCE})	-0.69 ± 0.01

Figure 4. Computer fitted polarisation curve with potential range ±100 mV at day 7 with averaged parameter values for extended potential range experiments.

Three sets of experiments were conducted under these new conditions. The cathodic controlling mechanism deduced for all OCP experiments was mixed activation/diffusion control, while the Tafel behaviour of the anodic branch mentioned is shown in Figure 4. The β_a value was fixed between a specific range while taking into account previous work done [9,10]. The corresponding table in Figure 4 gives the overall summarized parameter values. This translates to a corrosion rate (V_{corr}) of 248 ± 29 µm/yr. This correlates to aerated conditions in soil environment [10].

From observing the cathodic component behaviour (Figure 4), it tends towards a horizontal plateau. Therefore, the controlling mechanism was very close to pure diffusional control. The O_2 reached the electrode at a slow rate, but a pure diffusion regime was not completely attained. With time corrosion products formed, blocking the active electrode surface and thus increasing the E_{corr}. This was also consistent with the slight decrease in j_{corr} between day 2 and day 7 (not shown).

XRD diffractograms for coupons at OCP (Figure 5) show presence of lepidocrocite (L) and carbonated green rust (GR) with chemical makeup γ-FeO(OH) and $Fe^{II}_4Fe^{III}_2(OH)_{12}.CO_3$ respectively. GR is usually found in aerated conditions as illustrated by [12]. This points towards the availability of O_2 at the electrode vicinity. Aragonite (A) and calcite (C) were detected with Aluminum (Al). Al was observed because the sample holder is made up of Aluminum. Aragonite and calcite indicates the presence of active cathodic zones. This would explain why the electrode surface is not completely covered with L and GR, instead there are anodic and cathodic zones. The electrolyte allows easy formation of A and C and therefore these two species should be expected when cathodic polarization is applied.

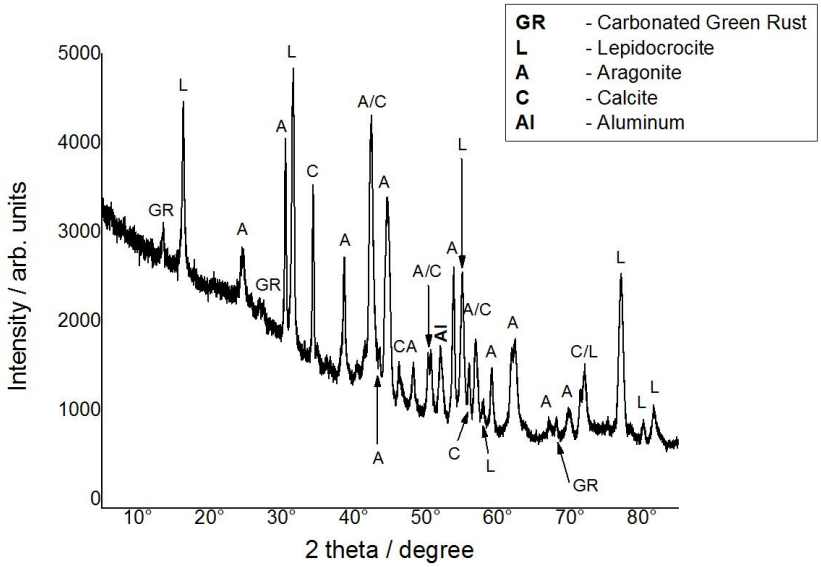

Figure 5. XRD diffractogram of products on coupons at OCP at the end of the experiment.

3.4. Anodic component

A true representation of the interfacial corrosion behaviour was obtained from the anodic component of the modelled polarisation curves. For this study the anodic component was compared for forward scans at day 7 by extrapolating the current density value at OCP [12]. As a basis and point of reference, the anodic component was also evaluated for modelled polarisation curves at OCP.

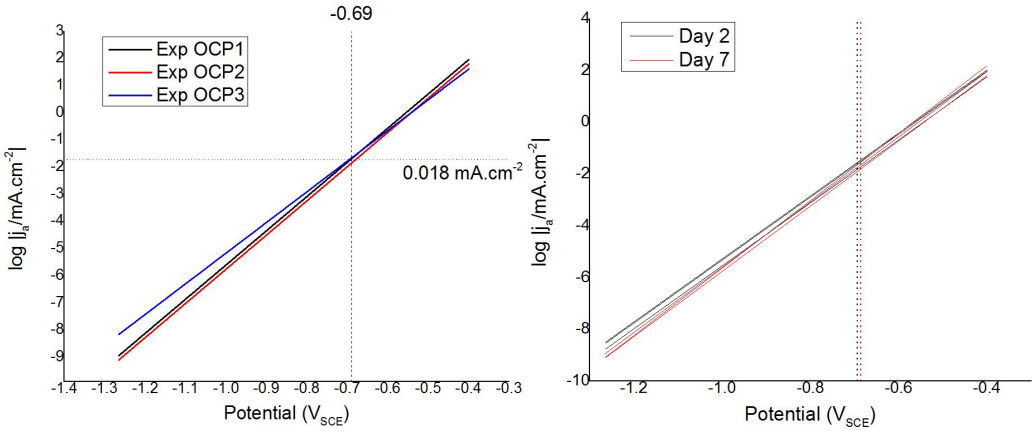

Figure 6. Anodic component for OCP experiments at day 7 for forward scans (A) and extrapolated current density from OCP anodic component (B)

The E_{OCP} was found to be –0.69 V_{SCE} of which the extrapolated anodic current density was 0.018 mA.cm^{-2} (see Figure 6A). This translates to a corrosion rate of 213 µm/yr. As a point of reference for cathodic protection anodic component analysis [12], the residual corrosion rate was predicted for applied cathodic potential –0.7 V_{SCE} to –1.2 V_{SCE} from the current density vs. potential curves (log|j_a| vs. E) in Figure 6. It can be deduced that when cathodic potential is applied at –0.8 V_{SCE}, the corresponding current density would be 0.008 mA/cm^2 and thus a residual corrosion rate of 14 µm/yr.

Interfacial corrosion behaviour can be directly related to the change in β_a values. This may be observed from the gradient of the anodic component as the gradient increases with time (Figure 6B). This behaviour may be due to the formation of corrosion products. The average EOCP for day 2 and 7 (–0.693 and –0.685 V_{SCE} respectively), represented by the vertical dotted lines, further validates this assumption. With time corrosion products form, blocking the active electrode surface and thus increasing the E_{corr}. The O_2 reaches the electrode at a slow rate but a pure diffusion was not completely attained. This is also consistent with the slight decrease in j_{corr} with time (not shown).

4. Conclusion

With the many parameters involved in the electrochemical system, the path travelled by current is one of the most crucial. Voltammetry around open circuit potential was carried out in order to understand interfacial behaviour without altering the metal/electrolyte interface. Formation of corrosion products on the metal surface resulted in slightly increased corrosion potential values with time. This may point towards the effects of perturbation of interface with time. A similar behaviour was observed with increased β_a values as they were observed to increase with time as depicted by anodic component graphs. The availability of O_2 at the metal/electrolyte interface was noted to be limited as the polarization curves showed limited O_2 diffusion behaviour.

Acknowledgement
This study is part of the collaborative Masters study at the University of Johannesburg and University of La Rochelle, carried out by Phumlani Mjwana and financially supported by the National Research Foundation (NRF) - South Africa

References

[1] Bahadori A. 8 - Commissioning of Cathodic Protection Systems. Cathodic Corrosion Protection Systems. Gulf Professional Publishing; 2014. 355-399
[2] Shi W, Lyon SB. Investigation using localised SVET into protection at defects in epoxy coated mild steel under intermittent cathodic protection simulating inter-tidal and splash zones. 2017 *Prog Org Coatings*. **102**:66–70
[3] Neville A, Morizot AP. Calcareous scales formed by cathodic protection - An assessment of characteristics and kinetics. 2002 *J Cryst Growth*. **243**(3–4):490–502.
[4] Barbalat M, Lanarde L, Caron D, Meyer M, Vittonato J, Castillon F, et al. Electrochemical study of the corrosion rate of carbon steel in soil: Evolution with time and determination of residual corrosion rates under cathodic protection. 2012 *Corros Sci*.;55:246–53
[5] Gabrielli C, Keddam M, Khalil A, Rosset R, Zidoune M. Study of calcium carbonate scales by electrochemical impedance spectroscopy. 1997 *Electrochim Acta*.
[6] Karoui H, Riffault B, Jeannin M, Kahoul A, Gil O, Ben Amor M, et al. Electrochemical scaling of stainless steel in artificial seawater: Role of experimental conditions on CaCO3and Mg(OH)2formation. 2013 *Desalination*. **311**:234–40.
[7] Ben Amor Y, Bousselmi L, Bernard MC, Tribollet B. Nucleation-growth process of calcium carbonate electrodeposition in artificial water-Influence of the sulfate ions. 2011 *J Cryst Growth*. **320**(1):69–77
[8] Kossakowski PG. Prediction of Ductile Fracture for S235JR Steel Using the Stress Modified Critical Strain and Gurson-Tvergaard-Needleman Models. 2012 *J Mater Civ Eng* **24**(12):1492–500.
[9] Rahal C, Masmoudi M, Abdelhedi R, Sabot R, Jeannin M, Bouaziz M, et al. Olive leaf extract as natural corrosion inhibitor for pure copper in 0.5 M NaCl solution: A study by voltammetry around OCP. 2016 *J Electroanal Chem* **769**:53–61
[10] Akkouche R, Rémazeilles C, Jeannin M, Barbalat M, Sabot R, Refait P. Electrochimica Acta In fl uence of soil moisture on the corrosion processes of carbon steel in arti fi cial soil : Active area and differential aeration cells 2016 *Electrochim Acta* **213**:698–708.
[11] Mahlobo MGR, Mjwana P, Tladi MNA, Obadele BA, Olubambi PA, Refait P. Evaluation of cathodic protection performance of carbon steel pipeline buried in soil: A review. In: Mechanical and Intelligent Manufacturing Technologies (ICMIMT), 2018 IEEE 9th International Conference on. IEEE; 2018. p. 37–43.
[12] Nguyen Dang D, Lanarde L, Jeannin M, Sabot R, Refait P. Influence of soil moisture on the residual corrosion rates of buried carbon steel structures under cathodic protection. Electrochim Acta. 2015;176:1410–9
[13] Barbalat M, Caron D, Lanarde L, Meyer M, Fontaine S, Castillon F, et al. Estimation of residual corrosion rates of steel under cathodic protection in soils via voltammetry. 2013 *Corros Sci* **73**:222–9
[14] Xiao-gang LI. Effect of Environmental Factors on Electrochemical Behavior of X70 Pipeline Steel in Simulated Soil Solution. 2009 *J Iron Steel Res Int* **16**(6):52–7.